An effective-medium theory approach to ordering in Cu-Au alloys

1992 J. Phys.: Condens. Matter 4 7191

(http://iopscience.iop.org/0953-8984/4/35/005)

J. Phys.: Condens. Matter 4 (1992) 7191–7202. Printed in the UK

An effective-medium theory approach to ordering in Cu–Au alloys

Zhigang Xi†, Bulbul Chakraborty†, Karsten W Jacobsen‡ and Jens K Nørskov‡

†Physics Department, Brandeis University, Waltham, MA 02254, USA

‡Laboratory of Applied Physics, Technical University of Denmark, DK-2800 Lyngby, Denmark

Received 8 May 1992

Abstract. We present a new approach, based on the effective-medium theory of metallic cohesion, to the study of alloy phase stability. The efficiency and applicability of the method is demonstrated by studying ordering in Cu–Au alloys. The ground-state properties of the three stoichiometric Cu–Au structures are found to be in excellent agreement with experiment. Monte Carlo simulations have been carried out in an effort to understand the finite-temperature phase transitions. These simulations give a very good description of the complete temperature–concentration phase diagram, and illustrate the importance of going beyond a fixed-lattice Ising model in describing phase transitions in these alloys.

One of the most fascinating problems in metal physics is that of alloy formation. Alloys exhibit a rich variety of structures as a function of temperature and concentration [1, 2] and there has been an intensive effort to understand alloy stability [3]. The problem has often been described by Ising models on a fixed lattice, and the statics and dynamics of these models have been extensively investigated [4, 5, 6]. In metals and semiconductors, the electrons play a crucial role in determining stability, and therefore it is of utmost importance to incorporate an accurate description of electronic structure into the construction of an alloy Hamiltonian [7]. Such approaches are usually based on density functional theory (DFT) which provides a formalism for calculating the ground-state energy of electrons for a given configuration of atoms [8].

In applying DFT, without further approximations, to alloys' phase diagrams, one is faced with the currently insurmountable task of calculating the energies of all possible alloy structures. In the search for simplification, a few different approaches have been developed, in all of which the interactions in the alloy Hamiltonian are derived by extrapolating from some known reference structures. One such approach is based on an accurate description of the *disordered* structures using the coherent potential approximation and the KKR scheme and the method of concentration waves to analyse ordering tendencies [7, 9]. The KKR–CPA approach has also been used to obtain the leading term of the Landau free energy functional describing a phase transition [7, 10], and, in conjunction with the cluster variation method, has been used to construct phase diagrams [11]. In another approach, the cluster interactions entering a generalized Ising model are constructed from accurate DFT total energy calculations

0953-8984/92/357191+12$04.50

of a set of ordered periodic structures [12, 13, 14]. Among other approaches, not based upon DFT, is a generalized Ising model derived from tight-binding calculations [3, 15].

In fixed-lattice Ising models, there is no coupling of the *structural* degrees of freedom to the configurational (Ising) degrees of freedom. The cluster interactions derived from DFT or tight binding are volume dependent, and the importance of this in determining phase stability has been emphasized in [12]. However, a complete treatment of the interplay between structural and configurational changes has so far remained beyond the scope of first-principles DFT-based calculations. In this paper we present an alternative DFT-based scheme which can treat these different variables on an equal footing.

The present approach is based on the effective-medium theory (EMT), which provides an efficient way of estimating the binding energy of a metallic system of atoms [16]. It is derived from DFT by making an *ansatz* for the electron density, $n(r) = \sum_i \Delta n_i(r)$, consisting of overlapping atomic densities $\Delta n_i(r)$ which are calculated in some reference system (the 'effective medium'). For each atom this reference system can be chosen as an atom embedded in a homogeneous electron gas of an appropriate density or an atom in the pure metal in a face-centred-cubic (FCC) structure with a suitable lattice constant. The success of the scheme in pure metals has been demonstrated through the study of a variety of different phenomena including surface relaxations, phonons [16], reconstructions [17] and premelting [18]. The related embedded atom method (EAM) has been applied successfully by Foiles *et al* and by Johnson to study the heat of solution in dilute alloys [19]. An *ab initio* approach based on the EMT density *ansatz* has been applied to pure metals. This method can be applied at various levels of approximations but does not rely on any experimental information [20]. The EMT Hamiltonian used for describing alloys in this work, relies on experimental information about the *ground-state* ($T = 0$) *properties* of a few ordered structures such as the pure metals and maybe one ordered compound. We are currently working on extending the *ab initio* scheme to alloys.

The major advantages of EMT are that (*a*) the method is essentially identical for pure metals and alloys, (*b*) since it can provide the binding energy of an arbitrary configuration of atoms, no *a priori* assumptions regarding the form of the alloy Hamiltonian need be made, and (*c*) the simplicity of the construction of the Hamiltonian makes it feasible to investigate the phase transformation properties through computer simulations. EMT has also proven to be very useful in constructing an atomistic Landau theory of alloys [21]. The analysis of this functional showed that EMT provides a very good description of all qualitative aspects of ordering in Cu–Au alloys, including the appearance of the CuAu-II phase, even within the mean-field picture [21]. The EMT approach also provides an efficient route, through Monte Carlo renormalization group calculations [22], to the construction of Ginzburg–Landau functionals for studying kinetics of phase transformations [23].

In the present work, we use simulations to study the finite-temperature phase transitions in the alloys of Cu and Au.

The key quantity that characterizes the binding energy of an atom in the EMT is the so-called *cohesive function* $E_{c,Z}(\overline{n})$. (There is one such function for each atomic number Z.) This is a simple function of the *embedding density* $\overline{n}$ of the atom, which is calculated as an appropriate average of the electron density coming from neighbouring atoms in the system. For a metal atom, $E_{c,Z}(\overline{n})$ exhibits a single minimum at some electron density n_0. This means that an atom can minimize its energy by seeking an environment with this electron density. The cohesive function

contains information about the volume dependence of the energy of the pure FCC metal: the cohesive energy of the metal is the minimum value of $E_{c,Z}(\overline{n})$, the equilibrium lattice constant is determined by the embedding density n_0, and the bulk modulus is proportional to the curvature of $E_{c,Z}(\overline{n})$. The cohesive function includes many-atom interactions because it is non-linear in the embedding density. It can be calculated as a function of embedding density for an atom in a homogeneous electron gas within the local density approximation [16, 24]. The estimates of the cohesive energy, the lattice constant, and the bulk modulus obtained in this way are typically within 10%, 5%, and 30%, respectively, of the measured values. In studying alloy properties, we choose to adjust the parameters in the cohesive function for each kind of atom (Cu and Au) to exactly reproduce the experimental values for the *pure* metals in the FCC structure, thus eliminating one obvious source of error in analysing phase diagrams. It should be emphasized that this choice is not essential to the method.

In the current EMT scheme, a neutral sphere is associated with each atom in the metallic system. In the atomic-sphere approximation (ASA), these spheres are assumed to be non-overlapping and space filling, implying a neglect of contributions coming from overlap of these neutral spheres. This is a reasonable approximation in close-packed structures of pure metals, and the binding energy, E_B^{ASA}, is given by the sum over the cohesive functions for all the atoms [16]

$$E_B^{(ASA)} = \sum_i E_{c,Z_i}(\overline{n}_i).$$

In dealing with alloys consisting of components with very different neutral sphere radii, or with open structures, the corrections to the ASA become important. As we shall see, these corrections are mainly responsible for driving the ordering transitions. Going beyond the ASA leads to an additional term in the binding energy, E_{AS}, which can be written as [16]

$$E_{AS} = \sum_i \alpha_i(\overline{n}_i - \overline{n}_i^{FCC}). \tag{1}$$

The first part, $\alpha_i\overline{n}_i$, is proportional to the embedding density and the coefficient α_i is the integral over a neutral sphere around atom i of the electrostatic potential from the charge density Δn_i associated with atom i. This is thus a measure of the electrostatic interaction of atom i with the electron tails from the neighbouring atoms. The second part, $-\alpha_i\overline{n}_i^{FCC}$, is a pair potential which exactly cancels the first part for a pure metal in a perfect FCC structure [16].

As with the cohesive functions, the parameters entering the atomic-sphere correction energy E_{AS} can be estimated from self-consistent calculations of an atom in a homogeneous electron gas but, just as in the case of E_c, we choose to adjust these in order to reproduce properties of the *pure* FCC metals. We call this model EMT_1 to distinguish it from a slightly modified version to be discussed later on.

In the construction of the energy expressions, simple analytic functional forms are used for the atomic electron density fall-off and for the cohesive functions. These functional forms have been discussed before [16] and mostly involve exponentials. This means that the evaluation of the binding energy involves pair sums of simple analytic functions and is, therefore, computationally very efficient.

The classical alloy Hamiltonian is the EMT binding energy written as a function of the continuous variables $\{R_i\}$, which define the positions of atoms, and the discrete, Ising-like, variables $\{\zeta_i\}$ which specify the type of atom i. The Hamiltonian can be written as;

$$H = \sum_i E_{c,Z_i}(\overline{n}_i(\{\zeta_j\},\{R_j\})) + \sum_i \alpha_i(\overline{n}_i(\{\zeta_j\},\{R_j\}) - \overline{n}_i^{FCC}(\{\zeta_j\},\{R_j\})). \quad (2)$$

The summations in this equation are over all atoms in the system.

In a fixed-lattice Ising model, the positions are *fixed* on a lattice and the occupation variables, defining whether a lattice site is occupied by a Cu atom or an Au atom, are the only degrees of freedom. The model cannot, therefore, describe changes in the positions of the atoms accompanying configurational ordering. These changes would be expected to affect the nature of transitions since, even at the level of global elastic deformations coupled to a nearest-neighbour Ising model, the behaviour is different from that of a rigid Ising model [25]. The work described here will be based on a Hamiltonian defined on a lattice but with the lattice parameters appearing as continuous variables. In this model, the variables $\{R_i\}$ are replaced by three independent lattice constants in equation (2). This describes a minimal model which takes account of the coupling between lattice deformations and configurational ordering. As is clear from equation (2), however, the EMT Hamiltonian does not have to be restricted to a lattice and work based on this complete Hamiltonian is now in progress. The minimal model has already led to new phenomena such as the appearance of the CuAu-II phase [21], and a change in the nature of the CuAu mean-field transitions from first to second order; the results of the Monte Carlo simulations, to be presented here, further demonstrate the differences with a fixed-lattice Ising model.

Before proceeding to the study of finite-temperature phase transitions, EMT was applied to study the ground-state properties of the the three stoichiometric compounds, Cu_3Au, CuAu, and $CuAu_3$. The results are summarized in table 1 and in figure 1(*a*). Comparing to both experiments and *ab initio* calculations, we see that EMT_1 gives a very good description of the variation of the lattice constant with composition [12, 14]. It describes the tetragonal distortion in the CuAu-I phase accurately, and the predicted trend in the formation energy agrees well with experimental data. However, EMT_1 generally overestimates the binding.

Figure 1(*a*) clearly demonstrates that a good description of the variation of the lattice constant with composition is essential for determining alloy properties. These volume effects are also present in DFT-based generalized Ising models [12]. We show in this work that with EMT, one can go one step beyond and investigate the effects of shape and symmetry changes on the phase diagram. As is clear from equation (2), EMT can describe vibrational and local relaxation effects [18] which have, so far, not been included in the simulation of alloys.

The EMT energy has two contributions: the cohesive functions and the atomic-sphere-correction energy which can, respectively, be viewed as the structural and configurational contributions to the energies of alloys. This is clearly illustrated in figure 1(*b*), which shows that the equilibrium volume and bulk modulus are mainly determined by E_c, whereas the heat of alloy formation is given primarily by E_{AS}. A similar analysis of the tetragonal distortion in CuAu shows that the c/a ratio is also determined by the cohesive function. This discussion indicates that a proper description of order–disorder transitions can only be obtained if both types of terms

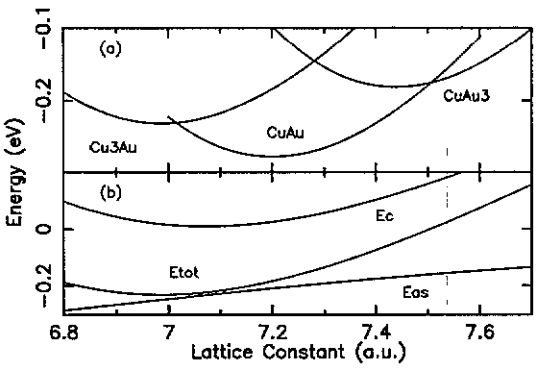

Figure 1. (*a*) Calculated binding energy (E_B) per atom relative to the energies of the elemental constituents for Cu_3Au, CuAu, and $CuAu_3$ shown as functions of the lattice constant. The results are given for the EMT_1 parameter set and the tetragonal distortion in the ordered CuAu structure is neglected. (*b*) Contributions of the cohesive energy E_c and the atomic-sphere correction E_{AS} to the ground-state energy of the ordered Cu_3Au structure shown as functions of the lattice constant.

Table 1. Calculated and experimental values for the lattice constant a, the tetragonal distortion parameter c/a, the formation energy E and the disordering temperatures T_c for the Cu–Au alloys obtained from Monte Carlo simulations in the canonical ensemble. The two experimental values of T_c for CuAu (658 K and 695 K) are for the CuAu-I and CuAu-II structures, respectively.

		EMT_1	EMT_2	Model A†	Model B‡	Expts §
	Cu_3Au	6.99	6.99	7.06	7.07	7.07
a (au)	CuAu	7.37	7.36	7.60	7.30	7.46
	$CuAu_3$	7.45	7.46	7.54	7.52	7.59¶
c/a	CuAu	0.93	0.93	0.90	1.0	0.93
	Cu_3Au	−0.231	−0.083	−0.036	−0.074	−0.074
E (eV)	CuAu	−0.288	−0.091	−0.063	−0.091	−0.091
	$CuAu_3$	−0.181	−0.044	−0.026	−0.059	−0.038
	Cu_3Au	1010	670	1146	942	663
T_c (K)	CuAu	910‖	708 (590‖)	950‖	886‖	658 695
	$CuAu_3$	790	480	677	698	≈ 500

†From [12] model A.
‡From [12] model B fitted to experimental parameters.
§Lattice constants from [2]; energies and temperatures from [30].
‖These values are calculated without the tetragonal distortion. Without this distortion EMT_1 gives $a = 7.20$, $E = -0.277$ and EMT_2 gives $a = 7.22$, $E = -0.082$.
¶Measured in disordered state.

are adequately represented. The figure also clearly demonstrates the source of the coupling, showing that ordering energies depend on the lattice constants which in turn are functions of the alloy configuration.

One of the important features of EMT is that the physical origin of the various terms entering the binding energy is known and therefore the origins of phase stability can be investigated. For example, one can analyse the striking asymmetry between the

formation energy of the $CuAu_3$ and Cu_3Au systems. We note from figure 1(*b*) that the cohesive function determines the equilibrium lattice constant and bulk modulus and E_{AS} determines the stability. This is true for all three systems $CuAu_3$, CuAu, and Cu_3Au. Furthermore the variation in E_{AS} is similar for Cu_3Au and $CuAu_3$. As seen in figure 1, the lattice constant for Cu_3Au comes out smaller than that for $CuAu_3$, simply because the Au electron density is more extended (due to the large 5d shell) than the Cu electron density. Since E_{AS} is more negative for the smaller lattice constants, the Cu_3Au structure becomes more stable than the $CuAu_3$ structure. The importance of volume effects on phase stability has been noted in [12] and the discussion above illustrates that these effects are included in EMT and that they can be easily analysed. The tetragonal distortion accompanying the appearance of long-range order in CuAu also has its origin in the cohesive energy term, since in this layered structure the Cu and Au atoms can better optimize the electron density of their environment by tuning this distortion.

As a first application of EMT to study finite-temperature phase transitions, Monte Carlo (MC) simulations were used to study the ordering transitions at the three stoichiometric compositions of Cu–Au. The space of positional degrees of freedom was restricted in this study to global changes of the lattice parameters. In this space, the state of an alloy can be described by the occupation variables $\{\zeta_i\}$, and the lattice parameters $\{a_\mu\}$, $\mu = 1, 2, 3$. Both of these sets were treated as independent random variables in our Monte Carlo simulations, and the calculated thermodynamic averages are based on the partition function

$$\mathcal{Z} = \prod_\mu \mathrm{d}a_\mu \sum_{\{\zeta_i\}} \exp(-\beta H(\{\zeta_i\}, \{a_\mu\})). \tag{3}$$

It should be emphasized that this partition function is not equivalent to that of an effective Ising model obtained from first-principles calculations. Even if one used calculated ground-state energies of all possible spin (alloy) configurations on a lattice, with the lattice constants optimized for every configuration, to construct the Ising Hamiltonian, this would be equivalent to making a saddle-point approximation to the a_μ integrals in the above partition function. No such approximation is made in our simulations and the fluctuations of the lattice parameters are taken into account in the same way as the fluctuations in the Ising variables $\{\zeta_i\}$. In the construction of the mean-field theory [21], the partition function is rewritten in terms of the order parameter describing configurational ordering, η

$$\mathcal{Z} = \int \mathrm{D}a_\mu \, \mathrm{D}\eta \exp(-\beta F(\eta, \{a_\mu\})) \tag{4}$$

and the mean-field approximation approximates $\mathcal{Z}$ by its saddle-point value obtained by minimizing the free energy functional F with respect to the lattice constants and the order parameter.

The study of the stoichiometric compositions was based on simulations performed using a canonical ensemble on an FCC lattice with periodic boundary conditions, since we were interested in a detailed analysis of the transitions at these fixed concentrations. In contrast, the construction of the complete phase diagram, to be described later, was based on simulations in the grand canonical ensemble. In the canonical ensemble simulations, downward temperature runs were performed to

identify ground-state structures, and both upward and downward runs were used to determine the ends of the hysteresis loop. The typical hysteresis loops in the canonical ensemble simulations were large and the transition temperatures, quoted in table 1, were defined to be the last temperature point, coming from the disordered side, at which *all* the error bars of the four sublattice populations intersect the line defining the average concentration [6]. The transition temperatures obtained from this definition will be seen to be consistent with the locations of the phase boundaries obtained from the grand canonical simulations.

Analysis of the CuAu transition shows clearly that ordering is accompanied by a tetragonal distortion (cf table 1). This feature could not have been captured by studying fixed-lattice Ising models with volume- and concentration-dependent interactions, and therefore, although first-principles calculations showed that the *ground state* of CuAu-I has tetragonal symmetry, effects of this on the phase transition could not be investigated [12]. The first-principles Ising model calculation did investigate the changes in volume accompanying the configurational ordering by minimizing the free energy with respect to both volume and spin configurations in the cluster variation method (CVM) calculation [12]. The atomistic Landau theory analysis [21] showed that the free energy functional for the situation where cubic symmetry was imposed was very different from the one where tetragonal distortions were allowed. In the former case the CuAu-I transition was predicted to be second order and in the latter it was predicted to be first order. Also, the gradient terms leading to the appearance of the CuAu-II phase were absent in the functional obtained for the cubic structure. This clearly indicates that the coupling to the tetragonal distortion is crucial in these systems.

In order to check the sensitivity of the results to parameters obtained by fitting to pure metals, and in an effort to see whether the agreement with experiment could be improved, we repeated our calculations with a slightly modified model. The atomic-sphere-correction energy, E_{AS}, involves two parameters; one specifying the strength of the interaction and the other the decay length. The E_{AS} energy in pure FCC metals involves only a product of these two parameters, whereas in alloys, the product and the decay length enter as two independent parameters. It is, therefore, possible to change the decay-length parameter without changing the description of the pure metals. By adjusting this parameter slightly for Cu so as to reproduce the experimental heat of formation of CuAu, we obtain a different Hamiltonian. We denote this model EMT_2. A complete discussion of the method and choices of parameters will be published elsewhere [27].

As can be seen from table 1, the results from EMT_1 and EMT_2 are very similar. The formation energies from EMT_2 agree much better with experiment and the values of T_c are also much closer to experiment. The fitting procedure employed in EMT_2 is similar to that of model B of [12]. However, in model B, the ground-state properties of all the stoichiometric compounds and the pure metals were fitted to experiment, whereas in EMT_2, only the properties of the pure metals and the formation energy of one ordered compound have been fitted. Moreover, the EMT Hamiltonian is never mapped onto an Ising model, and this is a crucial difference which manifests itself in the phase diagram obtained from the grand canonical simulations discussed later. Figure 2 shows the changes in the lattice constants and the variation of the long-range order parameter for the CuAu-I transition occurring in a $5\times5\times5$ (500-atom) lattice. These features remain unaltered in the larger simulations, but finite-size effects are observed and a new feature appears in simulations with sizes of $10\times10\times10$ or larger.

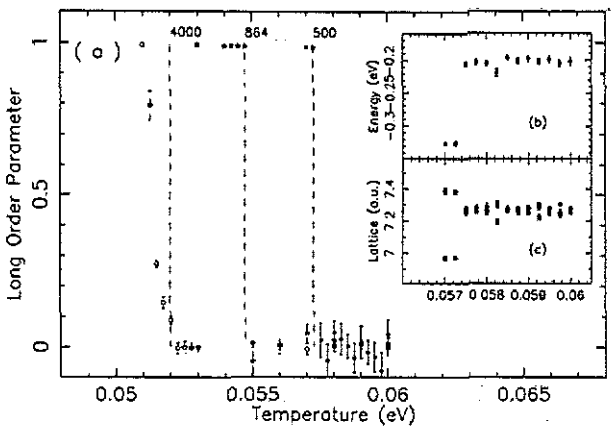

Figure 2. (*a*) Temperature dependence of the long-range order parameter for the CuAu-I structure. The insets show the variation with temperature of (*b*) the internal energy and (*c*) the lattice parameters, showing the increase of a_1 and a_2 and the decrease of a_3 at the transition to the ordered tetragonal CuAu-I structure. The data are from Monte Carlo simulations in a canonical ensemble taken during downward temperature runs starting from an initial random configuration at $T \gg T_c$ and using the EMT$_2$ parameters.

Since phase transitions can be defined unambiguously only for infinite systems, there is always a question of what can be deduced from finite-size simulations [26]. To monitor size effects, the simulations of the CuAu transition were repeated with larger numbers of atoms and the the finite-size scaling of T_c is shown in figure 3. We observe a size-dependent shift in the location of the transition. The shifts in T_c were seen to scale approximately inversely with volume as expected for a first-order transition [26]. This scaling implies that the uncertainties in the T_c values obtained from the 500-atom simulation are approximately 50 K, and that the results of the 4 000 atom simulation are very close to the infinite-volume limit.

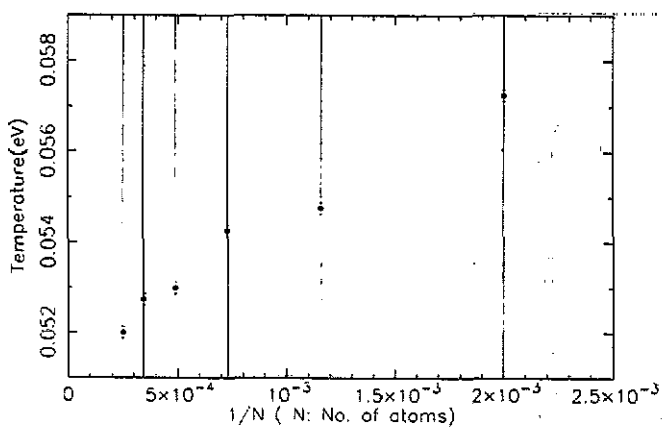

Figure 3. Finite-size scaling illustrated by size dependence of T_c for the CuAu-I transition. The transition temperature is seen to scale approximately as the inverse of the size (number of atoms) for sufficiently large systems.

The new feature to appear in the large simulations was the occurrence of

the CuAu-II phase, which is a long-period antiphase boundary structure with orthorhombic symmetry. The simulations on a fixed lattice with cubic symmetry show antiphase boundaries but an ordered antiphase boundary structure with the symmetry of the CuAu-II phase cannot, clearly, be observed in such simulations. The CuAu-II phase was characterized by a periodic spatial variation of the long-range order parameter along a direction perpendicular to the ordering direction [21], and by an orthorhombic distortion. Because of the large hysteresis effects inherent in the canonical simulations, and because of the narrow temperature range over which the CuAu-II phase is stable, it was difficult to isolate the disordered → CuAu-II and the CuAu-II → CuAu-I transitions in these simulations. The Landau theory of these transitions [21] predicts, to first order, transitions separated by 16 K. We are in the process of carrying out grand canonical simulations in systems larger than 4000 atoms, where the hysteresis effects are smaller, to pin down these transitions; the results will be presented in a future publication [28].

The results for the Cu_3Au and $CuAu_3$ transitions are shown in figure 4, where the long-range order parameters are plotted as a function of temperature. These simulations differ from the CuAu simulations in showing the presence of antiphase boundaries which are difficult to anneal out in a finite Monte Carlo run. This is the norm in Ising model simulations and the reason for the absence of antiphase boundaries in the CuAu simulation is quite possibly related to the lattice distortion which makes these defects energetically much less favourable. There is no distortion of the cubic symmetry in the Cu_3Au and $CuAu_3$ transitions, and since, in these simulations, we include only nearest neighbours in calculating the densities at atomic sites, the antiphase boundaries are zero-energy defects as in the nearest-neighbour Ising model.

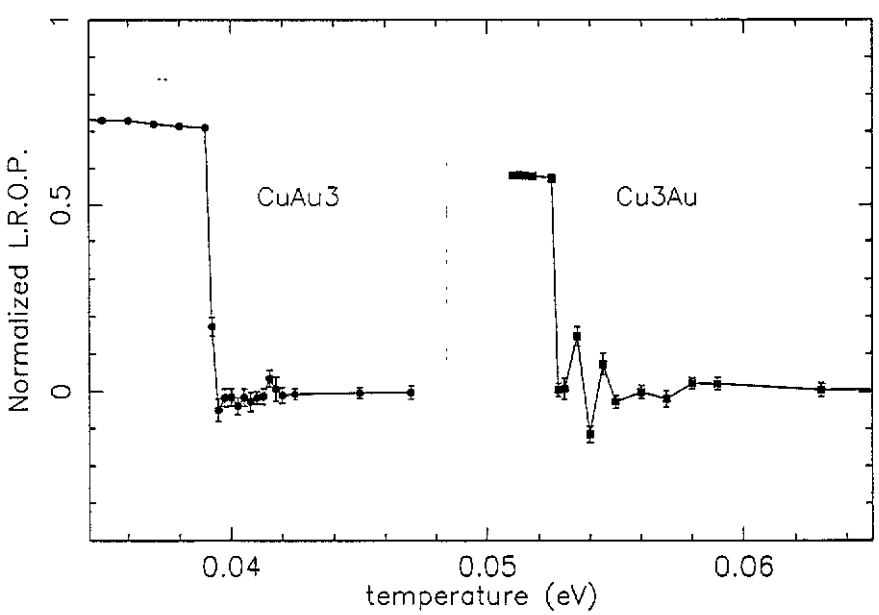

Figure 4. Long-range order parameters for Cu_3Au and $CuAu_3$ (cf text and description in figure 2 for details regarding the simulations).

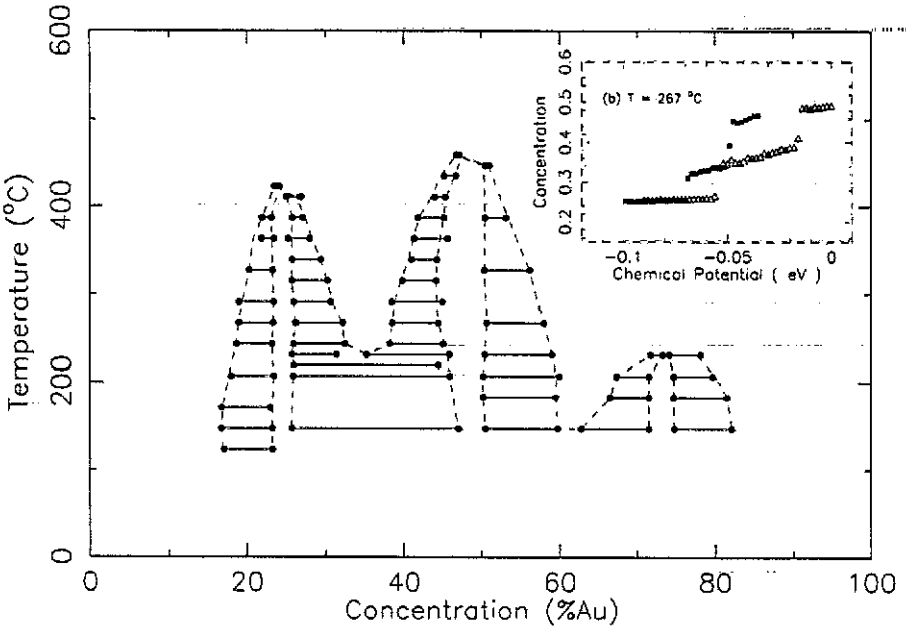

Figure 5. (*a*) Phase diagram obtained from a grand canonical simulation on a FCC lattice with variable lattice constants. The points mark the boundaries of the two-phase regions obtained from concentration versus chemical potential plots such as the one shown in the inset (cf discussion in text). The simulation box contained 500 atoms; periodic boundary conditions were imposed. The inset (*b*) shows a typical variation of average concentration with chemical potential. The triangles are for data taken during increasing chemical potential runs and the squares for decreasing chemical potential runs, and together they illustrate the hysteresis at the transitions. The data shown in the inset were obtained from runs of approximately 400 Monte Carlo steps per atom.

To map out the complete temperature concentration phase diagram for the Cu–Au system, we ran our Monte Carlo simulations in the grand canonical ensemble. In the thermodynamic limit, the results should not depend on the type of ensemble chosen. The demarcation of phase boundaries and two-phase regions can be accomplished more readily in a grand canonical simulation. The average concentration, calculated as a function of the chemical potential, shows discontinuities such as those shown in the inset of figure 5, at the temperature indicated in the figure. These mark the boundaries of the two-phase regions since it shows that no single-phase region exists in the concentration range between the limits of the jump [29]. The hysteresis loops at these chemical-potential-driven first-order phase transitions can be made very small by running the simulation for approximately 1000 MCS/atom. The phase diagram obtained from these simulations is shown in figure 5. The points mark the boundaries of the two-phase regions obtained from results such as those shown in the inset of figure 5. The agreement with experiment is very good in all respects except for the width of the two-phase regions. The relatively large width of the two-phase regions could be due to our neglect of local relaxations and phonons in calculating the phase diagram. The success of our model in reproducing the experimental phase diagram is, however, remarkable. The results shown were obtained from the 500-atom simulation and, hence, in the the absence of the CuAu-II phase. We plan to carry out larger

simulations in conjunction with our incorporation of local relaxations and vibrations into the scheme.

In conclusion, we have shown that the effective-medium theory provides an accurate description of the interactions in alloy systems, including the coupling of structural and configurational degrees of freedom, and thus goes beyond generalized Ising model descriptions. The ground-state properties and characteristics of order–disorder transitions are accurately reproduced, and the computational simplicity of the method makes it ideally suited for carrying out numerical simulations of equilibrium and non-equilibrium properties. In addition, the construction of EMT makes it possible to analyse the physical origins of the phase stability of alloys by formulating analytical schemes based on a first-principles Landau theory approach.

Acknowledgments

This work was supported in part by the grants DMR-9109264 and DMR-900034P.

References

[1] Hansen M 1958 *Constitution of Binary Alloys* (New York: McGraw Hill)
[2] Pearson W B 1958 *Handbook of Lattice Spacings and Structures of Metals* (New York: Pergamon)
[3] de Fontaine D 1979 *Solid State Physics* ed H Ehrenreich, F Seitz and D Turnbull (New York: Academic) vol 34 p 73
de Fontaine D 1986 *Electronic Band Structure and its Applications* ed M Yossouf (Berlin: Springer) and references therein
[4] Binder K P 1980 *Phys. Rev. Lett.* **45** 811
[5] Lebowitz J L, Phani M K and Styer D F 1985 *J. Stat. Phys.* **38** 413 and references therein
[6] Gahn U 1986 *J. Phys. Chem. Solids* **47** 1153
[7] Gyorffy B L, Johnson D D, Pinski F J, Nicholson D M and Stocks G M 1987 *Proc. NATO ASI Series on Alloy Phase Stability* (Dordrecht: Kluwer)
[8] Hohenberg H and Kohn W 1964 *Phys. Rev.* B **136** 864
[9] Gyorffy B L and Stocks G M 1983 *Phys. Rev. Lett.* **50** 374
[10] Pinski F J, Ginatempo B, Johnson D D, Staunton J B, Stocks G M and Gyorffy B L 1991 *Phys. Rev. Lett.* **66** 766
Staunton J B, Johnson D D and F J Pinski 1990 *Phys. Rev. Lett.* **65** 1259
[11] Turchi P E A, Sluiter M, Pinski F J, Johnson D D, Nicholson D M, Stocks G M and Staunton J B 1991 *Phys. Rev. Lett.* **67** 1779 and references therein
[12] Zunger A, Wei S H, Mbaye A A and Ferreira L G 1989 *Acta Metall.* **36** 2239
Wei S H, Mbaye A A, Ferreira L G and Zunger A 1987 *Phys. Rev.* B **36** 4163
[13] Connolly J W D and Williams A R 1983 *Phys. Rev.* B **27** 5169
[14] Terakura K, Oguchi T, Mohri T and Watanabe K 1987 *Phys. Rev.* B **35** 2169
[15] Turchi P, Sluiter M and de Fontaine D 1987 *Phys. Rev.* B **36** 3161 and references therein
[16] Jacobsen K W, Nørskov J K and Puska M J 1987 *Phys. Rev.* B **35** 7423
Jacobsen K W 1988 *Comment. Condens. Matter Phys.* **14** 129
[17] Jacobsen K W and Nørskov J K 1987 *The Structure of Surfaces II (Springer Series in Surface Sciences 11)* ed J F van der Veen and M A van Hove p 118
[18] Stoltze P, Nørskov J K and Landman U 1988 *Phys. Rev. Lett.* **61** 440
[19] Foiles S M, Baskes M I and Daw M S 1986 *Phys. Rev.* B **33** 7983
Johnson R A 1989 *Phys. Rev.* B **39** 12554
[20] Chetty N, Jacobsen K W and Nørskov J K 1991 *J. Phys.: Condens. Matter* **3** 5437
Chetty N, Stokbro K, Jacobsen K W and Nørskov J K 1992 preprint
[21] Chakraborty B and Xi Zhigang 1992 *Phys. Rev. Lett.* **68** 2039
[22] Binder K 1981 *Z. Phys.* B **43** 119
Kaski K, Binder K and Gunton J D 1984 *Phys. Rev.* B **29** 3996

[23] Gunton J D, San Miguel M and Sahni P S 1988 *Phase Transitions and Critical Phenomena* vol 8 ed C Domb and J L Lebowitz (Berlin: Springer)
Mazenko G F 1988 *Far From Equilibrium Phase Transitions* ed L Garrido (Berlin: Springer)
[24] Puska M J, Nieminen R M and Manninen M 1981 *Phys. Rev.* B **24** 3037
[25] Bergman D J and Halperin B I 1976 *Phys. Rev.* B **13** 2145
[26] Murty Challa S S, Landau D P and Binder K 1986 *Phys. Rev.* B **34** 1841
[27] Jacobsen K W and Nørskov J K to be published
[28] Xi Zhigang and Chakraborty B to be published
[29] Binder K, Lebowitz J L, Phani M K and Kalos M L 1981 *Acta Metall.* **29** 1655
[30] Hultgren R 1973 *Selected Values of the Thermodynamic Properties of Binary Alloys* (Metals Park, OH: American Society for Metals)
Orr R L 1960 *Acta Metall.* **8** 489